"Development And Characterization Of Transungual Drug Delivery System Consisting Of Nanosuspension Loaded Hydrogel Patches Of Terbinafine Hydrochloride (For The Treatment Of Onychomycosis)"

Ramdasi Bharat*, Dr. Jain Vikas¹, Gehalot Narendra², Malviya Yogendra³

Mahakal Institute of Pharmaceutical Studies, Dewas Road, behind Air Strip, Datana, Madhya Pradesh 456664

Onychomycosis is a common fungal infection affecting the nails, with a global prevalence of approximately 14%, especially impacting elderly individuals, diabetic patients, and those with compromised immune systems. This research focuses on developing an innovative transungual drug delivery system by incorporating terbinafine-loaded nanosuspensions into hydrogel patches. Terbinafine, a highly effective antifungal drug, faces challenges in topical application due to its poor water solubility and limited bioavailability. The formulation of nanosuspensions improves the drug's solubility, while the hydrogel patches enable sustained drug release and enhanced adhesion to the nail surface. The nanosuspension was prepared through high-pressure homogenization and characterized for particle size, zeta potential, and crystallinity. The hydrogel patches underwent evaluation for parameters including pH, mechanical strength, bioadhesive properties, and drug release behavior. Results demonstrated that this system significantly improved drug penetration, provided prolonged release, and exhibited potent antifungal effects. Overall, this strategy presents a promising, patient-friendly treatment option for onychomycosis with enhanced therapeutic efficacy.

Keywords: Transungual drug delivery; Nano-suspension; Hydrogel patch; Terbinafine.

¹Principal, MIPS, Ujjain, India

²Head of Department (Pharmaceutics), MIPS, Ujjain, India

³Associate Professor, MIPS, Ujjain, India

^{*}Student, MIPS, Ujjain, India

^{*} Corresponding author. Email: bharatramdasi5@gmail.com

1. INTRODUCTION:

Fungal infections represent a prevalent skin condition, especially in developing and underdeveloped regions, impacting over 40 million individuals globally. Among these, superficial fungal infections rank as one of the most frequently encountered conditions in clinical practice. Various fungal species, including dermatophytes, Tinea pedis, and yeast strains, are responsible for causing these superficial infections. The intensity of fungal infections can vary widely depending on factors such as the infection site, the specific fungal pathogen involved, and the individual's personal hygiene and health habits. Over the past thirty years, numerous antifungal agents have been developed and categorized into several classes. The most common topical antifungal groups include Azoles, characterized by an imidazole ring structure, and Allylamines, which contain amine functional groups [1].

1.1 Nails

Nails are specialized structures distinct from bone, composed primarily of keratin—a tough, fibrous protein also found in hair and the outermost layer of the skin. They serve a protective function, shielding the fingertips and surrounding tissues from physical trauma^[2].

Fig. 1 shows the human fingernail located at the far end of each finger. Nails are part of the body's skin appendages, alongside hair and glands. They develop from the epidermis, the skin's outer layer, and are made up of tiny cells known as onychocytes. These cells contain large amounts of keratin, a protein that gives nails their strength and hardness^[2].

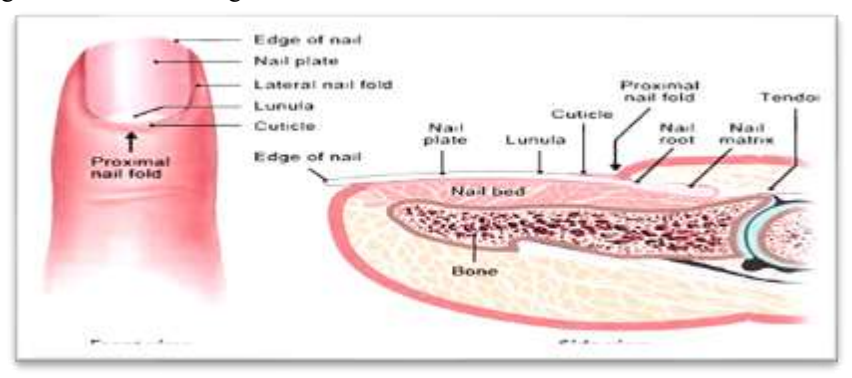


Fig 1: Structure and Anatomy of Nails

1.1.1 Nails Diseases

Although nail disorders are generally not life-threatening, they can cause significant pain, discomfort, and unsightly appearance for those affected. These conditions may result in substantial physical limitations, impacting daily activities and work, as well as psychological and emotional distress. In some cases, damaged or deformed nails can harm the surrounding tissues, increasing the risk of secondary bacterial infections. Nail diseaseas refer to medical conditions that impact the fingernails or toenails^[3].



Fig 2: Onychomycosis

1.2 Transungual Drug Delivery system

The term "transungual" is derived from "trans," meaning "through," and "unguis," meaning "nail." Thus, a transungual drug delivery system refers to a method of administering medication through the

nail to specifically target nail-related conditions. Due to the nail's natural hardness and low permeability, it presents a significant barrier, making drug delivery through this route challenging^[3]. In transungual drug delivery, the medication embedded in a topical formulation penetrates the nail plate and gradually moves into deeper layers, potentially extending to the nail bed (refer to Fig. 3)^[4].



Fig 3: Transungual delivery and key factors that determine its efficacy

1.2.1 Nanosuspension-Loaded Hydrogel Patches in Transungual Drug Delivery

a. Definition and Concept

A nanosuspension is a submicron colloidal system containing drug particles (typically under 500 nm) dispersed in a liquid medium and stabilized using surfactants or polymers. Meanwhile, a hydrogel patch is a moisture-rich, polymer-based film capable of adhering to the nail surface, facilitating sustained drug delivery^[5].

b. Advantages of This Approach

- Localized therapy minimizes systemic exposure and adverse effects
- Non-invasive alternative to oral antifungals
- Improved drug permeability through the nail
- Increased patient compliance due to ease of application and reduced dosing
- Sustained drug release ensures prolonged therapeutic levels at the site of infection^[6].

1.3 Drug Profile

Terbinafine hydrochloride is a **synthetic allylamine antifungal agent**, widely used to treat **fungal infections of the skin and nails**, including **onychomycosis** and **dermatophytosis**. Marketed under the brand name **Lamisil**, it is especially effective against dermatophytes and other common fungal pathogens. It was granted FDA approval on **December 30, 1992**^[7].

Fig 4: Structure of Terbinafine

a. Indications

Terbinafine HCl is prescribed for the treatment of infections caused by:

• Trichophyton species (e.g., T. rubrum, T. mentagrophytes)

- Epidermophyton floccosum
- Microsporum canis
- Tinea species
- Yeasts such as Candida species
- Lipophilic fungi like Malassezia furfur^[7]

b. Mechanism of Action

Terbinafine acts by blocking the activity of the enzyme squalene epoxidase (also referred to as squalene monooxygenase), which plays a key role [8].

- Inhibition of this enzyme blocks the conversion of squalene to 2,3-oxidosqualene, disrupting cell membrane formation^[8].
- As a result, there is a reduction in ergosterol synthesis and an accumulation of intracellular squalene, leading to increased membrane permeability and ultimately fungal cell death^[8].
- Additionally, the buildup of squalene may cause the formation of squalene-containing vesicles that disturb the cytoplasmic lipid balance, further weakening the fungal cell wall^[8].

c. Pharmacodynamics

- Terbinafine is highly lipophilic, allowing it to accumulate in the skin, nails, and adipose tissues, enhancing its efficacy in superficial fungal infections.
- It exhibits a long terminal elimination half-life, supporting once-daily dosing and prolonged antifungal action.
- Due to its wide therapeutic index, the drug is generally well-tolerated even at higher doses. However, baseline liver function tests (LFTs) are recommended prior to initiating oral therapy to minimize the risk of hepatotoxicity.

d. Toxicity and Overdose

- The subcutaneous LD₅₀ in laboratory animals (rats and mice) is greater than 2 g/kg, indicating relatively low acute toxicity.
- In humans, the TDLO (Toxic Dose Low) reported in women is approximately 210 mg/kg over six weeks.
- Although overdose cases are rare, symptoms may include:
- Nausea and vomiting
- Abdominal discomfort
- Treatment of overdose typically involves activated charcoal administration and supportive symptomatic care^[9].

2. MATERIAL AND METHOD

2.1. Material

A. Materials/Chemicals used in Investigation

The chemicals used in the present study were procured from reputed sources to ensure analytical grade quality and reliability. Terbinafine hydrochloride was obtained as a gift sample from Bioplus Life Science, Bangalore. Common laboratory reagents including sodium chloride, sodium hydroxide, and triethanolamine were purchased from S. D. Fine Chem. Ltd., Mumbai. Hydrochloric acid, potassium dihydrogen phosphate, methanol, pluronic F-68, propylene glycol, glycerine, urea hydrogen peroxide, and polyvinyl alcohol were sourced from Loba Chemie Pvt. Ltd., Mumbai. Sodium dihydrogen phosphate was procured from Hi Media Pvt. Ltd., Mumbai. Ethanol, carbopol 934, and chloroform were supplied by Sunkem, India. Additionally, Pluronic F-127 was obtained from S. D. Fine Chem. Ltd., Mumbai. All chemicals were of analytical grade and used without further purification.

B. Instruments Used in Investigation

The instruments employed in the present research work were sourced from reliable manufacturers to ensure precision and accuracy in experimental procedures. A UV-visible spectrophotometer from Shimadzu was used for absorbance measurements, while the Fourier Transform Infrared (FTIR)

spectrophotometer was procured from Bruker, Germany, for identifying functional groups. Mechanical stirring during formulation was carried out using a Remi mechanical stirrer. Optical observations were made using an optical microscope from Lyzer, Ambala, and centrifugation was performed using a micro centrifuge from REMI Laboratory, Mumbai. For in vitro drug release studies, a Franz diffusion cell from Electro Lab., Mumbai was utilized. The pH of formulations was measured using a pH meter from Accumax India, New Delhi.

Weighing procedures were conducted using an electronic balance from Contech Instruments Ltd., Mumbai, which also supplied the melting point apparatus. A hot air oven from Oracle Equipments, New Delhi, and a vacuum oven from Ajanta were used for drying processes. Thermal analysis was performed using a Differential Scanning Calorimeter (DSC) from Perkin-Elmer India Pvt. Ltd., Thane. Moisture content was determined using an IR moisture balance from Scope Enterprises, New Delhi. Transmission electron microscopy (TEM) was conducted using a high-resolution microscope from Hitachi, Tokyo, Japan, and particle size analysis was carried out using an instrument from Malvern Instruments, UK. Lastly, the preparation of nanosuspensions involved the use of a probe sonicator from Athena Technology, Thane.

2.2. Method

2.2.1 Preformulation Studies

Initial characterization of Terbinafine was conducted to assess its suitability for formulation:

- **Organoleptic properties**: Terbinafine was observed for its physical appearance, color, and odor to confirm its identity and detect any abnormalities.
- Melting point: Determined using a melting point apparatus to assess purity and stability.
- **Solubility profile**: Solubility was examined in solvents including distilled water, methanol, ethanol, and phosphate buffers of different pH to aid in solvent and formulation selection.
- UV spectral analysis: The drug's maximum absorbance wavelength (λ -max) was identified in various solvents, crucial for further spectrophotometric analysis.
- Calibration curves: Standard curves were plotted in methanol, water, and buffer solutions to determine linearity and concentration range for analytical quantification.
- FT-IR and DSC analysis: FT-IR spectroscopy was used to confirm the functional groups and identity of the drug, while DSC was used to study the thermal behavior and compatibility with excipients.
- **Partition coefficient**: Calculated to understand drug lipophilicity, which impacts permeation through biological membranes.
- Moisture content: Determined using an IR moisture balance to evaluate hygroscopicity and stability.

2.2.2 Formulation of Terbinafine Nanosuspension

Terbinafine nanosuspensions were developed using the solvent evaporation followed by ultrasonication method to obtain nanosized drug particles with improved dispersion and stability. In this process, terbinafine hydrochloride was dissolved in methanol (25 mL) at ambient temperature. This drug solution was then slowly injected into 50 mL of aqueous surfactant solution containing different concentrations of Pluronic F-68 and Pluronic F-127, which had been pre-filtered using a 0.45 μ m membrane filter^[10]. To preserve the stability of the formulation, the injection was carried out while maintaining the receiving aqueous phase at 4°C using an ice bath. The resulting mixture was gently stirred using a magnetic stirrer for 2.5 hours, allowing the methanol to evaporate gradually. For optimal dispersion, organic solvent addition was done via syringe directly into the surfactant solution, ensuring controlled mixing^[10].

Following complete evaporation of the organic phase, the coarse suspension was further subjected to probe ultrasonication under varying intensities to reduce the particle size and achieve a uniform nanosuspension.

This method ensured the formation of stable terbinafine nanosuspensions suitable for incorporation into hydrogel patches^[10].

2.2.3 Characterization of Nanosuspension

- Particle Size and PDI: One of the primary assessments involved the determination of particle size and polydispersity index (PDI) using dynamic light scattering (DLS). This technique provided insights into the average size of the nanoparticles and the distribution range, which are critical factors influencing drug release and bioavailability. A lower PDI value indicated a more uniform particle distribution, suggesting a stable and well-dispersed nanosuspension system^[11].
- Zeta Potential Measurement Zeta potential measurement was then carried out to assess the surface charge of the nanosuspension particles. The zeta potential reflects the electrostatic repulsion between particles in suspension, and its value is a key indicator of colloidal stability. Higher absolute values (either positive or negative) of zeta potential generally suggest good stability by preventing particle aggregation due to repulsive forces^[11].
- Saturation Solubility Testing nano suspension was evaluated in different solvents to determine the extent of solubility enhancement achieved through nanosizing. The increase in surface area due to reduced particle size contributes significantly to improved dissolution behavior, which is particularly advantageous for poorly water-soluble drugs. This study confirmed the improved solubility profile of the drug in the nanosuspension form compared to its pure form^[11].
- **Drug content** This was achieved by subjecting the nanosuspension to centrifugation to separate the nanoparticles from the dispersion medium, followed by dilution and analysis using UV-Visible spectrophotometry. The results confirmed the presence and stability of the drug within the nanosuspension, indicating successful formulation^[11].

2.2.4 Preparation of Hydrogel Patches

The nanosuspension was incorporated into hydrogel patches as follows:

Hydrogel-based patches were formulated using the optimized terbinafine nanosuspension identified from earlier evaluations. The patch matrix was designed using Carbopol 934 as the gelling agent, with PVA and urea hydrogen peroxide (UHP) included to enhance structural integrity and nail penetration. To begin, Carbopol 934 was dispersed in distilled water with constant stirring and allowed to hydrate completely. Separately, PVA was dissolved in warm water (70–80°C), and its concentration was varied across formulations to study its effect on film-forming ability and mechanical strength^[12]. Once the PVA solution cooled, it was combined with the hydrated Carbopol mixture. Propylene glycol, used as a plasticizer and humectant, was also added in varying amounts to optimize flexibility and moisture retention. UHP was incorporated into the blend as a keratolytic agent to improve transungual drug permeation. Triethanolamine was used to adjust the pH to facilitate gelling and maintain compatibility with skin and nail tissues^[12]. The final formulation was cast onto a flat, non-stick surface and dried at controlled temperature (40–45°C) until a flexible, uniform film was formed. These dried films were carefully cut into patches of standardized size and stored for further evaluation^[12].

2.2.5 Evaluation of Nanosuspension-Loaded Hydrogel Patches

- Physical characteristics: The physical characteristics of the patches were first assessed through visual inspection to check for uniformity in appearance, absence of air bubbles or cracks, and overall transparency. Uniformity in weight was checked using an analytical balance, and surface smoothness was assessed both visually and by touch to confirm an even texture among other things such as thickness using Vernier caliper and content uniformity in %, which is crucial for comfort and adhesion and overall evaluation^[13].
- **Bioadhesion testing:** Bioadhesive strength, a vital parameter for ensuring prolonged contact with the nail surface, was determined using a texture analyzer. In this test, a hydrogel patch was affixed to a probe and brought into contact with a nail substrate under standardized pressure for a specific time. The force required to detach the patch from the nail was recorded, indicating its adhesive potential. Strong bioadhesion ensures that the patch remains securely in place during application, thereby enhancing drug permeation without causing discomfort or trauma to the nail bed^[13].
- pH measurement: The pH of the hydrogel patches was measured to ensure compatibility with the
 physiological pH of the nail and surrounding skin. A known quantity of the patch was dispersed in
 distilled water and allowed to swell, after which the pH was measured using a calibrated pH meter.

Maintaining the pH within the range of 5.0 to 7.5 was essential to minimize the risk of irritation and ensure biocompatibility^[12, 13].

- In-vitro drug release: In-vitro drug release studies were performed to evaluate the release profile of the drug from the hydrogel matrix. Franz diffusion cells were used for this purpose, with the patch placed in the donor compartment and a synthetic membrane separating it from the receptor compartment filled with phosphate buffer (pH 7.4). The drug content was analyzed using a validated analytical technique such as UV-Visible spectro-photometry or HPLC. The cumulative drug release was plotted against time, and various kinetic models including zero-order, first-order, Higuchi, and Korsmeyer-Peppas were applied to understand the release mechanism^[13].
- Ex-vivo permeation studies: Ex-vivo permeation studies were carried out to evaluate the ability of the drug to penetrate through the nail plate under conditions that mimic real-life clinical scenarios. These studies employed human cadaver nails or animal nail models, such as porcine hooves, which closely resemble the structure of the human nail. The hydrogel patch was applied to the dorsal surface of the nail tissue mounted in a Franz diffusion cell. Over specified time intervals, samples were withdrawn from the receptor compartment and analyzed for drug concentration. This study provided valuable insight into the drug's ability to traverse the nail barrier, which is critical for effective treatment of conditions such as onychomycosis^[13].

3. RESULTS AND DISCUSSIONS

3.1 Findings from Preformulation Experiments

3.1.1 Organoleptic properties:

Using organoleptic evaluation, Terbinafine Hydrochloride was found to be a white fine crystalline powder with no discernible odor, confirming its expected physical attributes.

3.1.2 Melting Point Observation

The melting point was determined using a standard melting point apparatus. The drug exhibited a melting range between 210°C and 230°C, indicating the substance was in a pure state with no observable signs of decomposition.

3.1.3 Solubility Profile

To evaluate the solubility, the shake-flask method was utilized. Terbinafine exhibited significant solubility in methanol (~402 mg/mL), moderate solubility in ethanol and phosphate buffer pH 7.2, and was practically insoluble in water. These observations justified the application of nanosizing to improve solubility and bioavailability.

Table 01: Qualitative solubility of Terbinafine

| Solvent used | Solubility of Terbinafine |
|------------------------|---------------------------|
| Distilled water | |
| 0.1N hydrochloric acid | + |
| Ethanol | ++++ |
| Methanol | ++++ |
| Chloroform | +++ |
| 0.1N NaOH | ++ |
| Phosphate buffer 7.2 | +++ |
| Phosphate buffer 5.5 | +++ |

3.1.4 Spectroscopic and Calibration Data

Using UV spectroscopy, the absorption maximum (λ -max) was identified at **283 nm**. Calibration curves generated in various solvents exhibited good linearity within the chosen concentration range (5–50 μ g/mL), validating the method's reliability for further drug content analysis.

A. Findings and Interpretation

I. Wavelength of Maximum Absorbance (λ-max)

The peak absorbance (λ -max) was consistently observed at 283 nm in both methanol and phosphate buffer pH 7.2. This confirms the ideal detection wavelength for terbinafine in subsequent spectrophotometric studies.

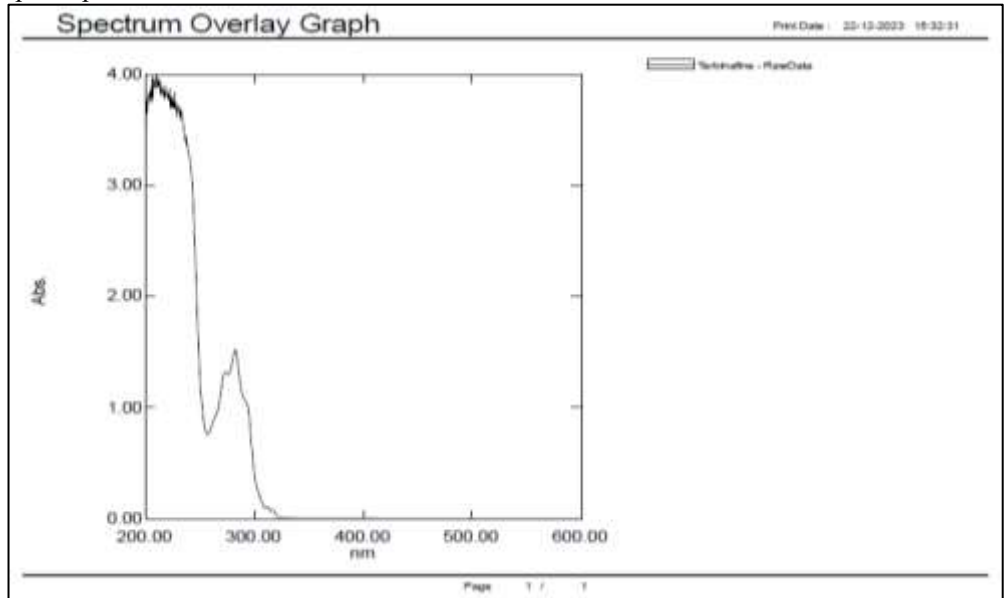


Fig 5: Wavelength maxima of Terbinafine in methanol

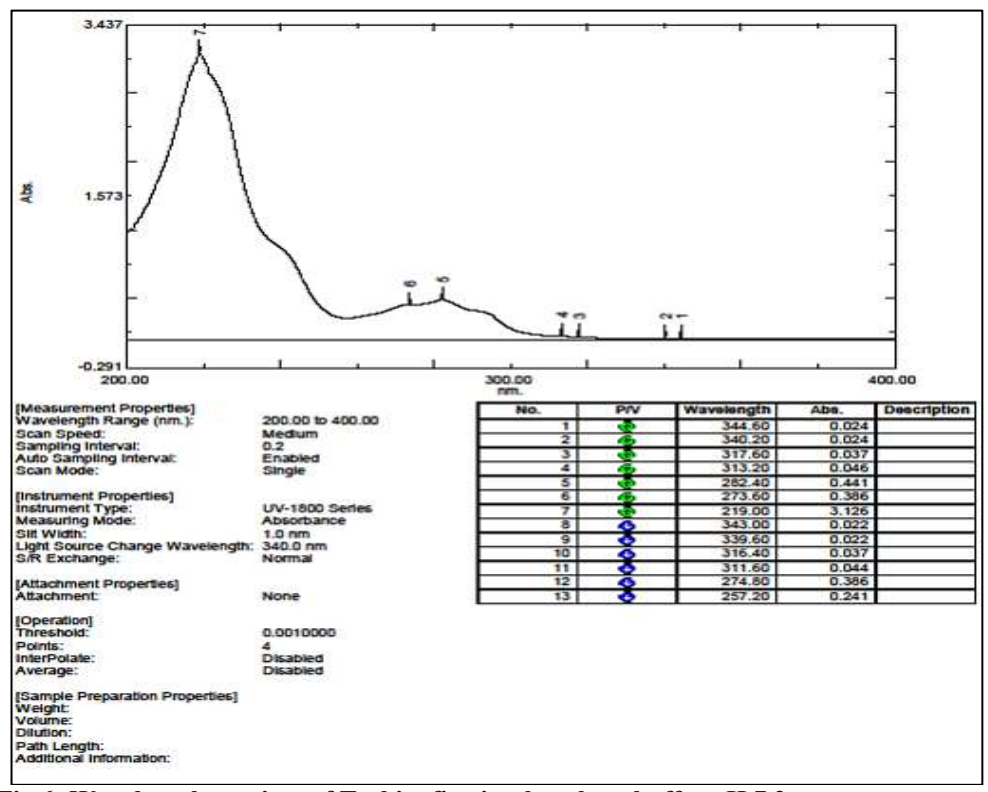


Fig 6: Wavelength maxima of Terbinafine in phosphate buffer pH 7.2

3.1.5 Calibration Curve Data

a) In Methanol (Concentration: 10–50 μg/mL):

The absorbance increased linearly with concentration:

Table 02: Calibration curve of Terbinafine in methanol

| Concentration (µg/mL) | Mean Absorbance |
|-----------------------|-----------------|
| 10 | 0.270 |
| 20 | 0.494 |
| 30 | 0.712 |
| 40 | 0.945 |
| 50 | 1.161 |

(Mean \pm SD; n=3)

The curve showed excellent linearity, confirming the reliability of quantification in methanol.

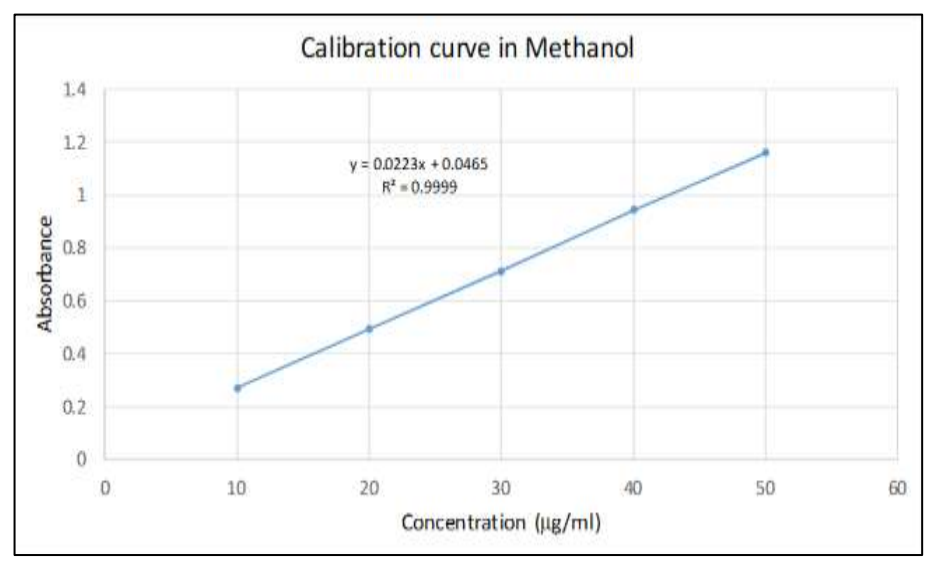


Fig 7: Calibration curve of Terbinafine in methanol b) In Phosphate Buffer pH 5.5:

Table 03: Calibration curve of Terbinafine in phosphate buffer pH 5.5

| Concentration (µg/mL) | Mean Absorbance |
|-----------------------|-----------------|
| 10 | 0.329 |
| 20 | 0.501 |
| 30 | 0.665 |
| 40 | 0.836 |
| 50 | 1.040 |

(Mean \pm SD; n=3)

This buffer system also demonstrated a strong linear trend, making it suitable for further use in permeation and release studies.

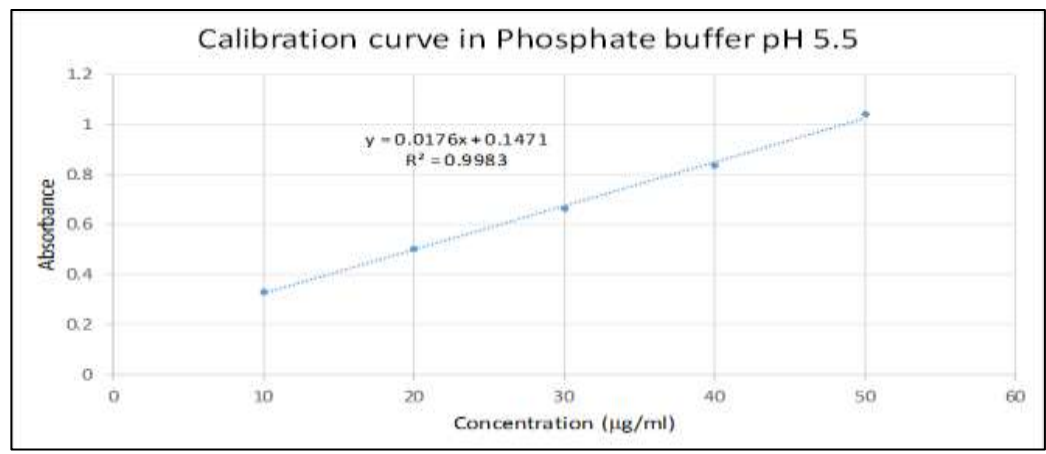


Fig 8: Calibration curve of Terbinafine in phosphate buffer pH 5.5

c) In Phosphate Buffer pH 7.2:

Table 4: Calibration curve of Terbinafine in phosphate buffer pH 7.2

| Concentration (µg/mL) | Mean Absorbance |
|-----------------------|-----------------|
| 5 | 0.175 |
| 10 | 0.347 |
| 15 | 0.513 |
| 20 | 0.701 |
| 25 | 0.873 |

(Mean \pm SD; n=3)

This medium was found optimal for simulating physiological nail conditions. The curve again displayed strong linearity ($R^2 \approx 0.999$), confirming method accuracy.

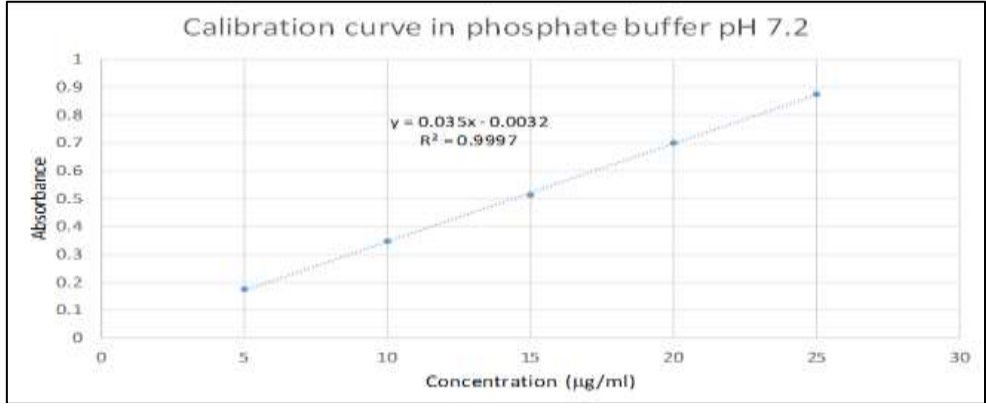


Fig 9: Calibration curve of Terbinafine in phosphate buffer pH 7.2 d) In Water:

Table 5: Calibration curve of Terbinafine in water

| Concentration (μg/mL) | Mean Absorbance |
|-----------------------|-----------------|
| 10 | 0.154 |
| 20 | 0.323 |
| 30 | 0.554 |
| 40 | 0.775 |
| 50 | 0.987 |

(Mean \pm SD; n=3)

Though linear, absorbance values were lower due to terbinafine's low solubility in water. This emphasized the drug's need for formulation strategies like nanosuspensions to improve solubility.

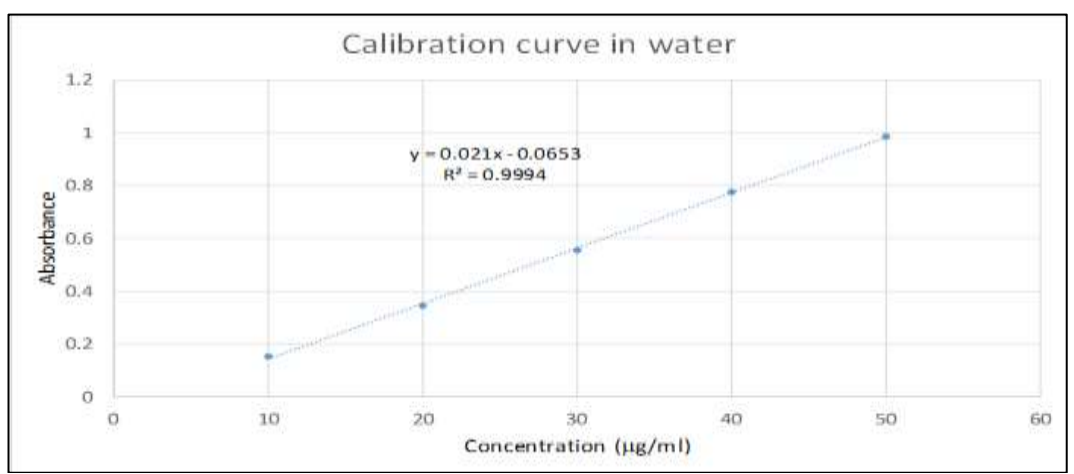


Fig 10: Calibration curve of Terbinafine in water Conclusion from UV Analysis

- λ -max = 283 nm (consistent across solvents).
- Calibration curves were linear across all mediums tested.
- Best absorbance and solubility occurred in methanol and phosphate buffer pH 7.2.
- These results validated the spectrophotometric method for accurate quantification of terbinafine in various formulations and studies.

3.1.6 FT-IR and DSC analysis:

The FTIR spectrum of **pure Terbinafine Hydrochloride** displayed sharp, well-defined absorption peaks corresponding to functional groups in its chemical structure:

- N-H stretching (secondary amine): seen around 3300 cm⁻¹, Showing the presence of amine groups.
- C-H stretching (alkyl and aromatic): seen at approximately 2900 cm⁻¹, consistent with the aliphatic chains.
- C=C stretching (aromatic ring): seen near 1600 cm⁻¹, confirming the aromatic nature of the molecule.
- C-N and C-S stretches: noted around 1200-1300 cm⁻¹ and 600-700 cm⁻¹, validating the presence of amine and thioether functionalities.

When compared with the FTIR spectra of physical mixtures of the drug and excipients (Carbopol 934, Pluronic F-68, Triethanolamine), no major peak shifts, disappearance, or new peaks were observed. This indicates that no chemical interaction or incompatibility occurred between Terbinafine and the selected formulation ingredients.

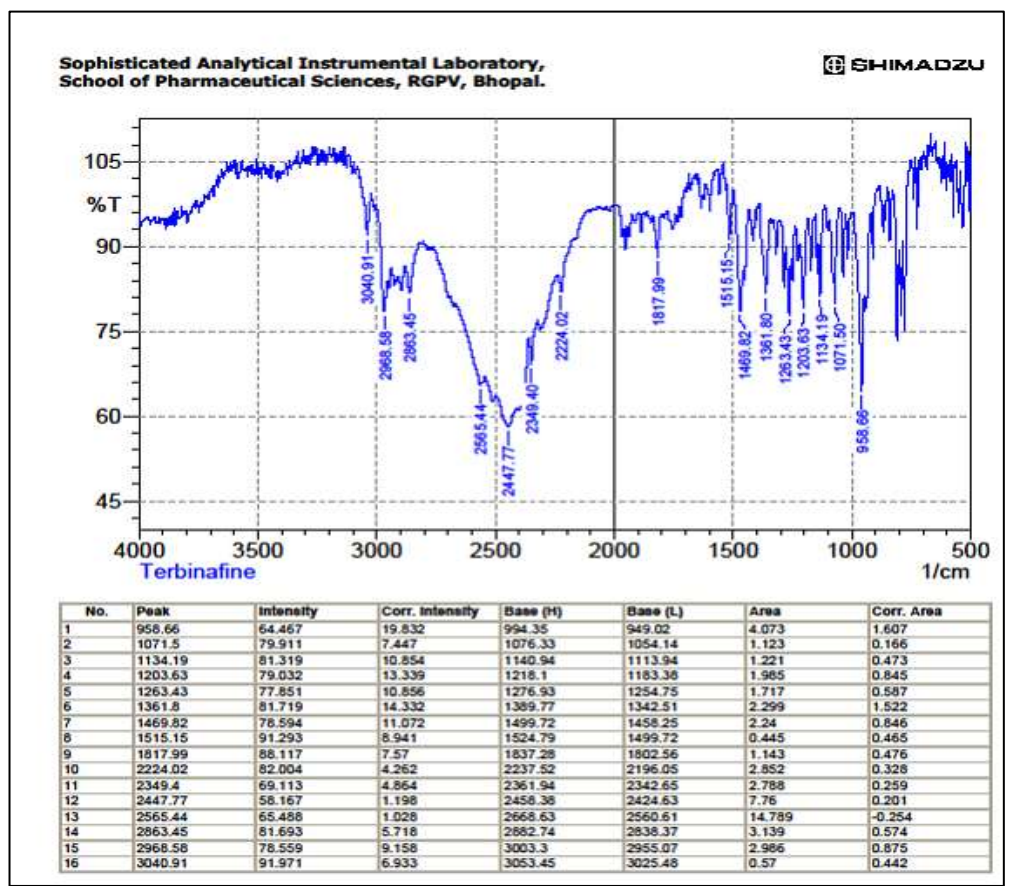


Fig 11: FTIR identification graph of Terbinafine HCl

• Conclusion:

The FTIR study confirmed:

- The identity of Terbinafine based on its functional group peaks.
- Excellent physicochemical compatibility with the chosen excipients, justifying their use in nanosuspension and hydrogel formulations.

The DSC thermogram of Terbinafine Hydrochloride showed a distinct, sharp endothermic peak at approximately 215–225°C, which corresponds to its melting point. The sharpness of the peak indicates that the drug is highly crystalline in nature. No additional thermal events were detected, implying absence of polymorphic transformation or thermal degradation within the analyzed range.

Moreover, when compared with the thermograms of drug-excipient mixtures, the melting peak of Terbinafine remained intact, with no significant shift or broadening. This further confirms that the drug remained stable and did not undergo any chemical or physical interaction upon mixing with formulation components.

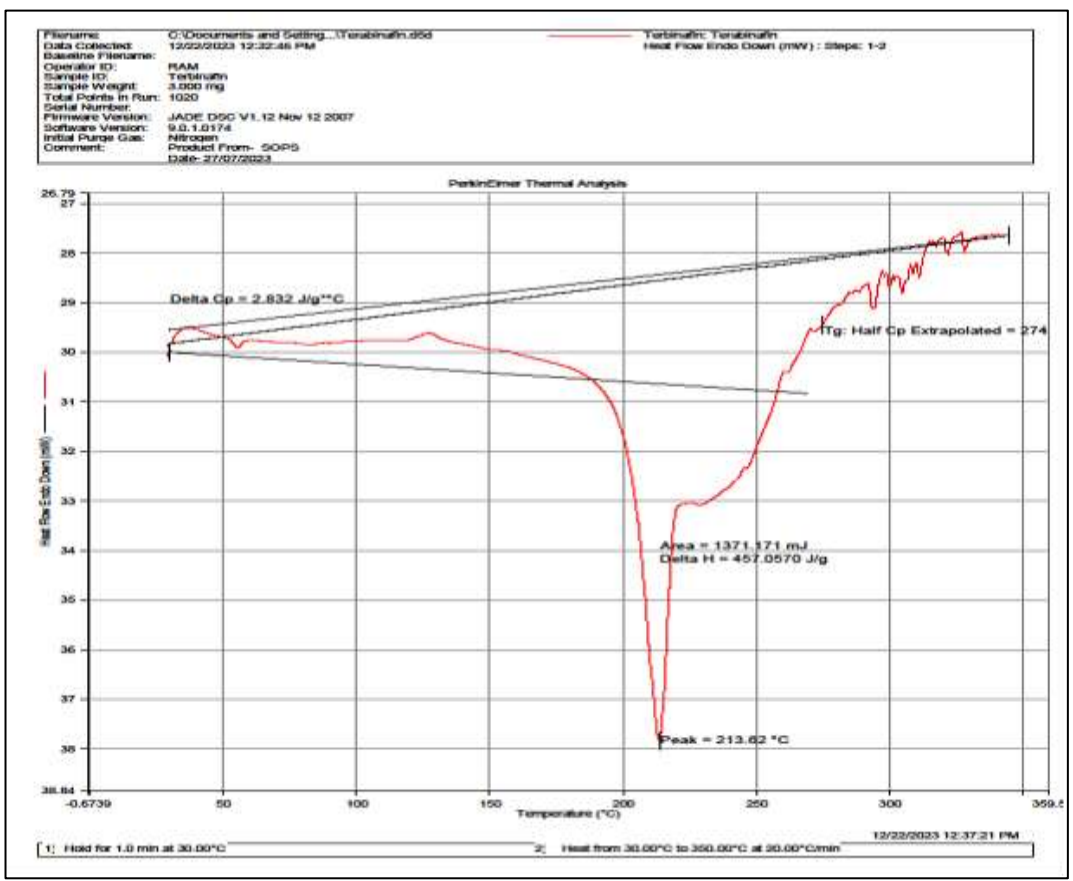


Fig 12: DSC Identification graph of Terbinafine HCl

• Conclusion:

The DSC study established that:

- o Terbinafine is **thermally stable** up to its melting point.
- o It exists in a **crystalline form**, suitable for formulation.
- o No thermal incompatibilities were observed with the excipients used.

3.1.7 Partition coefficient and moisture content

Table 6: Partition coefficient of Terbinafine

| S.No. | Volume of Aqueous | Volume of Organic | Concentration in Aqueous phase | Concentration in Organic phase | $logP = log10(P_{organic} /$ |
|--------|-------------------|----------------------|--------------------------------|--------------------------------|------------------------------|
| | phase (ml) | phase (ml) | (μg/ml) | (μg/ml) | Paqueous) |
| 1. | 50 | 50 | 69.28 | 1298.20 | 1.27 |
| 2. | 50 | 50 | 54.93 | 1450.67 | 1.42 |
| 3. | 50 | 50 | 63.00 | 1042.60 | 1.22 |
| Averag | | | | | 1.30 |
| e | | | | | |

Moisture Content

The moisture content was found to be less than 1.5%, indicating that the drug was relatively dry and free from hygroscopic behavior under normal laboratory conditions. This low moisture level helps ensure chemical stability and enhanced shelf-life of the bulk drug during storage and handling.

Table 7: Moisture content determination

| S.No. | Drug | KF Factor | Amount of KF Reagent consumed | Moisture content |
|-------|------------------------------|-----------|----------------------------------|---------------------|
| 1. | Terbinafine hydrochloride | 0.311 | 0.15 ml | 0.046 |

3.2 Characterization and Evaluation of Nano suspension

The formulated nanosuspension underwent the following evaluations:

3.2.1 Particle size:

Particle sizes varied from 228.6 nm (F6) to 696.4 nm (F1) across batches. F6 and F8 emerged as the most optimal formulations in terms of particle size reduction.

Table 8: Particle Size Results

| F. code | Z average size (nm) | Temperature (°C) |
|-----------------------|---------------------|------------------|
| F ₁ | 334.4 ± 45.2 | 25 |
| F ₂ | 467.9 ± 22.9 | 25 |
| F ₃ | 264 ± 42.1 | 25 |
| F ₄ | 696.4 ± 21.7 | 25 |
| F ₅ | 668.8 ± 43.5 | 25 |
| F ₆ | 228.6 ± 25.9 | 25 |
| F ₇ | 371.7 ± 27.2 | 25 |
| F ₈ | 310 ± 16.7 | 25 |

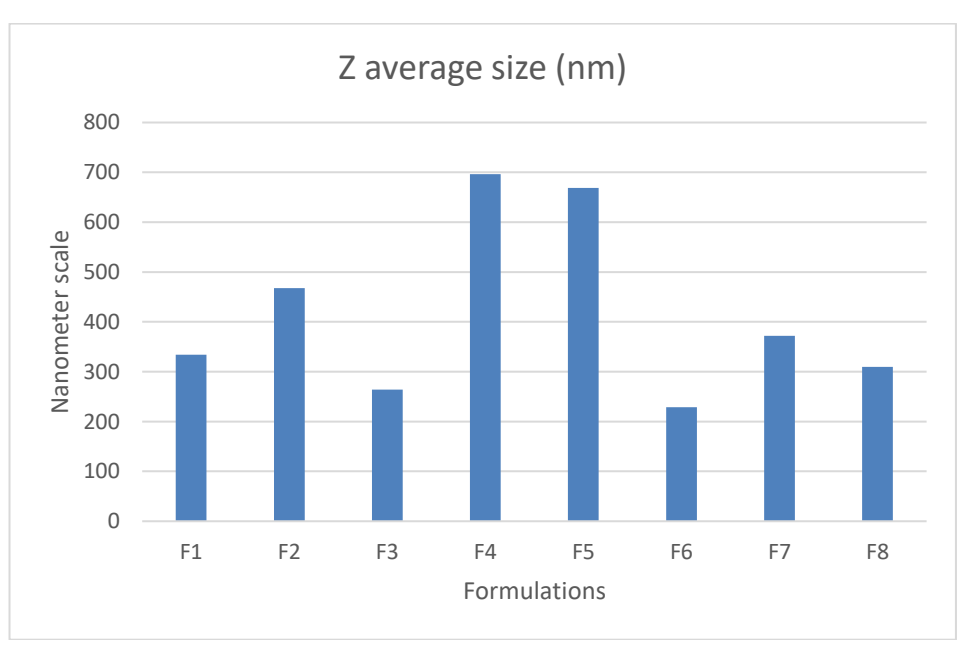


Fig 13: Graph for Particle Size

3.2.2 Zeta potential

The surface charge, which indicates colloidal stability, was measured for all formulations:

• Zeta potential values ranged between -11.2 mV (F6) and +24.8 mV (F7).

• These moderately high values suggest the formulations were **electrostatically stable**, with minimal risk of particle aggregation.

| Table 9: Zeta p | ootential Results |
|-----------------|-------------------|
|-----------------|-------------------|

| Formulation code | Zeta Potential (mV) | Temperature (°C) |
|-----------------------|---------------------|------------------|
| \mathbf{F}_1 | 2.8 | 25.0 |
| F ₂ | 2.8 | 24.9 |
| F ₃ | 0.2 | 25.0 |
| F ₄ | 5.9 | 25.0 |
| F ₅ | 21.3 | 25.1 |
| F ₆ | -11.2 | 25.0 |
| F ₇ | 24.8 | 25.1 |
| F ₈ | 15.0 | 24.9 |

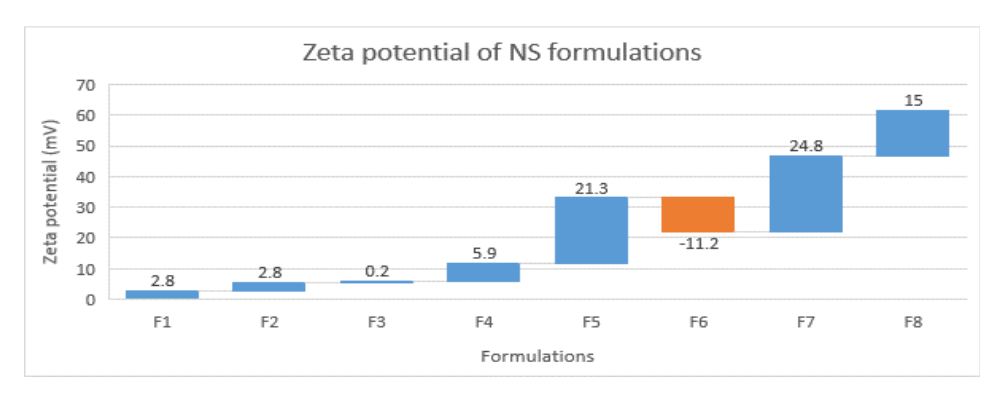


Fig 14: Visual representation of Zeta potential of various NS formulations

3.2.3 Saturation solubility

The nanosized drug demonstrated significantly improved solubility in aqueous media compared to the pure drug:

The highest saturation solubility was observed in F4 (11.9 \pm 0.13 mg/mL) and F8 (10.37 \pm 0.18 mg/mL). The improved solubility is likely a result of the smaller particle size and greater surface area produced by the ultrasonication process.

Table 10: Saturation solubility of Terbinafine HCl Nanosuspensions

| Formulation code | Particle size (nm) | Saturation solubility (mg/ml) |
|------------------|--------------------|-------------------------------|
| $\mathbf{F_1}$ | 334.4 | 8.87 ± 0.25 |
| \mathbf{F}_{2} | 467.9 | 8.04 ± 0.37 |
| F ₃ | 264.0 | 8.85 ± 0.21 |
| F ₄ | 696.4 | 11.9 ± 0.13 |
| F ₅ | 668.8 | 8.06 ± 0.27 |
| \mathbf{F}_{6} | 228.6 | 8.93 ± 0.33 |
| F ₇ | 371.7 | 8.8 ± 0.43 |
| F ₈ | 310.0 | 10.37 ± 0.18 |

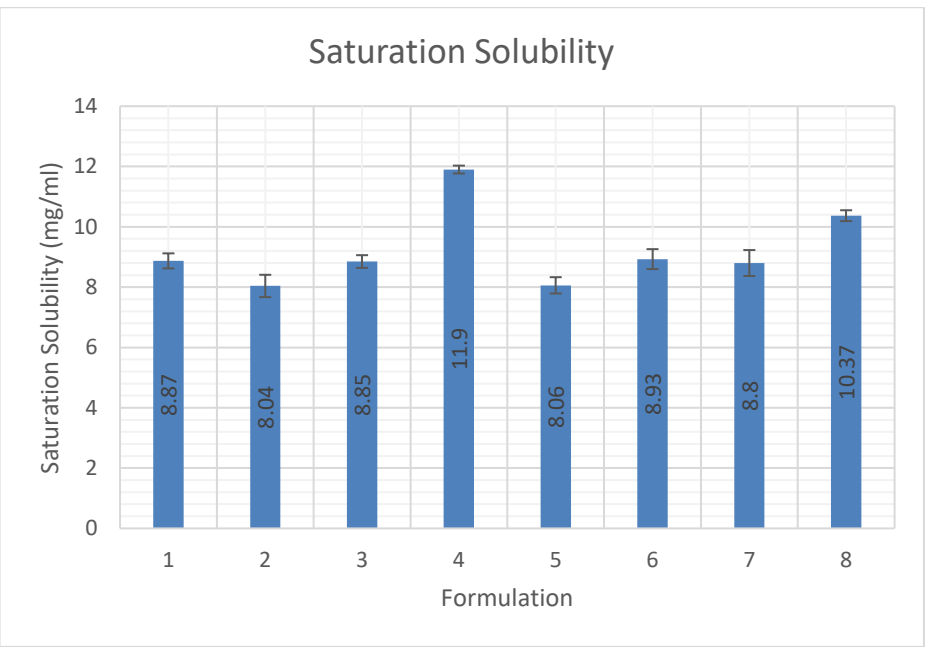


Fig 15: Visual representation of saturation solubility of various NS formulations

3.2.4 Drug Content

Spectrophotometric analysis revealed variations in drug content across formulations:

- Values ranged from 2.0 ± 1.3 mg/mL (F2) to 8.49 ± 1.22 mg/mL (F8).
- The high content in F8 suggests efficient incorporation of drug during formulation and minimal drug loss during processing.

Table 11: Total Drug Content of Terbinafine HCl Nanosuspensions

| Formulation code | Particle size (nm) | Total Drug Content (mg/ml) |
|-----------------------|--------------------|----------------------------|
| F ₁ | 334.4 | 5.81 ± 1.45 |
| \mathbf{F}_2 | 467.9 | 2.27 ± 1.24 |
| F ₃ | 264.0 | 2 ± 1.3 |
| F ₄ | 696.4 | 6 ± 2.53 |
| F ₅ | 668.8 | 5.23 ± 1.13 |
| F ₆ | 228.6 | 7.33 ± 1.21 |
| F ₇ | 371.7 | 7.55 ± 0.34 |
| F ₈ | 310.0 | 8.49 ± 1.22 |

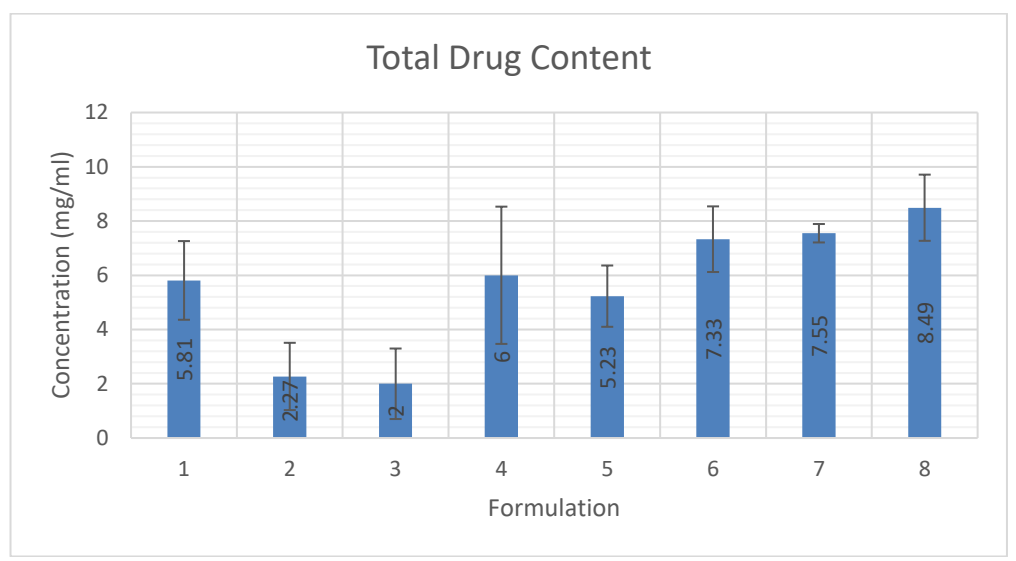


Fig 16: Visual representation of total drug content of various NS formulations

3.3 Evaluation of Nanosuspension-Loaded Hydrogel Patches

The final hydrogel patches were subjected to extensive analysis, including:

3.3.1 Physical characteristics

• Visual Appearance

The formulated gel patches presented a **smooth, white, and non-gritty appearance**, with no visible phase separation or crystal formation. The uniform consistency indicated proper dispersion of the nanosuspension within the gel matrix.

The weight variation data of the patches are as follows;

Table 12: Results of Appearance of hydrogel patch formulations

| Formulation Code | Appearance |
|------------------|---------------|
| 1 | White, opaque |
| 2 | White, opaque |
| 3 | White, opaque |
| 4 | White, opaque |
| 5 | White, opaque |
| 6 | White, opaque |
| 7 | White, opaque |
| 8 | White, opaque |
| 9 | White, opaque |

• Thickness and Weight Consistency

Table 13: Results of Thickness of hydrogel patch formulations

| Formulation Code | Thickness (mm) |
|------------------|----------------|
| 1 | 1.6 ± 0.18 |
| 2 | 1.8 ± 0.02 |
| 3 | 2 ± 0.17 |

| 4 | 1.8 ± 0.21 |
|---|----------------|
| 5 | 2.1 ± 0.02 |
| 6 | 1.9 ± 0.19 |
| 7 | 1.7 ± 0.11 |
| 8 | 1.8 ± 0.17 |
| 9 | 2.2 ± 0.06 |

Table 14: Results of Weight variation of hydrogel patch formulations

| Formulation Code | Weight (gram) |
|------------------|------------------|
| F1 | 2.96 ± 0.329 |
| F2 | 3.21 ± 0.315 |
| F3 | 3.35 ± 0.318 |
| F4 | 3.62 ± 0.284 |
| F5 | 3.45 ± 0.32 |
| F6 | 3.59 ± 0.229 |
| F7 | 3.32 ± 0.233 |
| F8 | 3.46 ± 0.281 |
| F9 | 3.67 ± 0.261 |

Measurements using a Vernier caliper revealed patch thickness values between 1.6 ± 0.18 mm and 2.2 ± 0.06 mm, while weight varied from 2.96 ± 0.32 g to 3.67 ± 0.26 g. These minimal fluctuations suggest that the patches were cast uniformly and consistently across batches.

• Content Uniformity test

Spectrophotometric assays confirmed consistent Terbinafine distribution across all gel patches, with only minor deviations from the intended drug concentration. This indicates efficient dispersion of the nanosuspension during the formulation process.

Table 15: Results of content uniformity of hydrogel patch formulations

| Formulation Code | Content Uniformity (%) |
|------------------|------------------------|
| 1 | 101.1 ± 0.351 |
| 2 | 99.48 ± 0.159 |
| 3 | 102.11 ± 0.386 |
| 4 | 99.39 ± 0.217 |
| 5 | 99.17 ± 0.108 |
| 6 | 99.9 ± 0.272 |
| 7 | 98.97 ± 0.361 |
| 8 | 99.63 ± 0.191 |
| 9 | 98.86 ± 0.145 |

3.3.2 Bioadhesion testing

Formulations F6 to F9 displayed excellent adhesive qualities (+++), ensuring strong adherence to the nail surface throughout the application period.

| Formulation Code | Adhesiveness |
|------------------|--------------|
| 1 | - |
| 2 | + |
| 3 | ++ |
| 4 | ++ |
| 5 | ++ |
| 6 | +++ |
| 7 | +++ |
| 8 | +++ |
| 9 | +++ |

Table 16: Results of Adhesion of hydrogel patch formulations

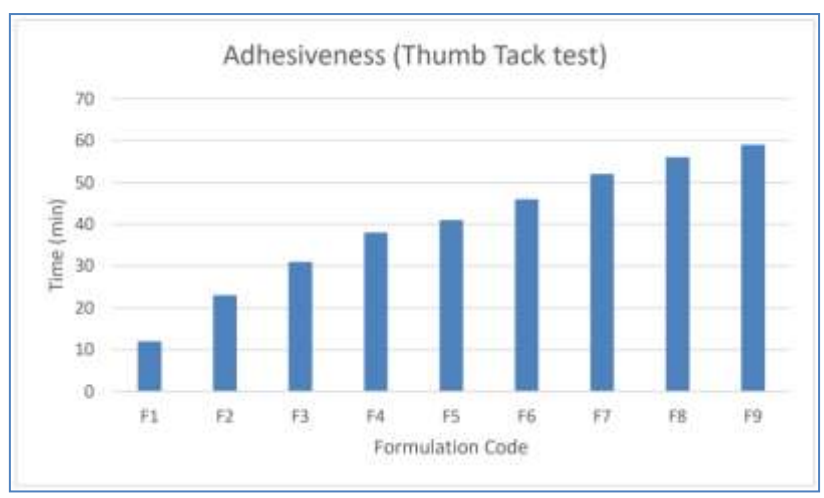


Fig 17: Graphic presentation of Thumb Tack test

3.3.3 pH measurement

pH values align well with the acceptable physiological pH for skin and nail applications, suggesting that the formulation is unlikely to cause irritation upon use.

Table 17: Results of pH of hydrogel patch formulations

| Formulation Code | pН |
|------------------|------|
| 1 | 6.69 |
| 2 | 6.73 |
| 3 | 6.85 |
| 4 | 6.74 |
| 5 | 6.64 |
| 6 | 6.58 |
| 7 | 6.78 |
| 8 | 6.80 |
| 9 | 6.87 |

3.3.4 In-vitro Drug Release Study

The in-vitro drug release of the optimized nano suspension-loaded hydrogel patch formulation F7 was evaluated using a Franz diffusion cell, with dialysis membrane as a semi-permeable barrier. The study was conducted in phosphate buffer pH 7.4 at 37 ± 0.5 °C for 8 hours.

Formulation F7 exhibited a **rapid and sustained release profile**, with an initial burst release of **10.79%** within the first 5 minutes (0.083 h), and a cumulative drug release of **99.35%** at the end of 8 hours — the highest among all formulations tested. This indicates excellent permeability and matrix hydration, suitable for transungual delivery.

• Kinetic Modeling (In-vitro Data):

Formulation F7 showed the best fit with the **Zero Order model** ($R^2 = 0.9982$), suggesting a constant release rate. The **Korsmeyer–Peppas model** showed an **n-value of 0.72**, indicating **anomalous (non-Fickian) diffusion**, where both diffusion and swelling influence drug release. The release rate constant k = 0.237, confirming F7 as the **fastest releasing formulation**.

Table 18: Results of in-vitro diffusion studies of hydrogel patch formulations

| Time | F1 | F2 | F3 | F4 | F5 | F6 | F7 | F8 | F9 |
|-------|-------------|---------------|---------------|---------------|-------------|---------------|-------------|---------------|---------------|
| (h) | (μg/ | (μg/ml) | (μ g / | (μ g / | (μg/ | (μ g / | (μg/ | (μ g / | (μ g / |
| | ml) | | ml) | ml) | ml) | ml) | ml) | ml) | ml) |
| 0.083 | 20.9 | 13.6 ± | $6.83 \pm$ | 23.93 | 19.83 ± | 12.1 ± | 37.77 ± | 29 ± | $24.14 \pm$ |
| | ± 0.12 | 0.12 | 0.4 | ± 0.07 | 0.4 | 0.48 | 0.07 | 0.12 | 2.03 |
| 0.166 | 25.1 ± | 17 ± 0.12 | 8 ± 0.12 | 29 ± | 23 ± | 13.43 | 40 ± | 30 ± | $27.5 \pm$ |
| | 0.4 | | | 0.12 | 0.36 | ± 0.3 | 0.12 | 0.12 | 1.21 |
| 0.25 | $29.53 \pm$ | 33.43 ± | $11.17 \pm$ | 33.43 | $27.83 \pm$ | 16.6 ± | $43.97 \pm$ | $33.27 \pm$ | $29.4 \pm$ |
| | 0.08 | 0.08 | 0.96 | ± 0.08 | 0.03 | 0.12 | 0.74 | 0.08 | 0.12 |
| 0.5 | 34 ± | $37.4 \pm$ | $15.87 \pm$ | $38.5 \pm$ | 31.6 ± | $29.2 \pm$ | $58.73 \pm$ | $55.6 \pm$ | $33.1 \pm$ |
| | 0.48 | 0.12 | 0.74 | 0.48 | 0.09 | 0.36 | 0.08 | 1.21 | 0.26 |
| 1 | $45.23 \pm$ | $44.67 \pm$ | $32.33 \pm$ | 47.53 | $35.93 \pm$ | 35.57 | $74.1 \pm$ | $62.93 \pm$ | $44.13 \pm$ |
| | 0.08 | 0.4 | 0.08 | ± 0.74 | 2.41 | ± 0.74 | 0.36 | 0.3 | 0.08 |
| 2 | 80.1 ± | $70.17 \pm$ | 54.6 ± | 69.67 | 59.73 ± | 56.17 | 97.5 ± | $83.9 \pm$ | $66.47 \pm$ |
| | 0.12 | 0.3 | 0.12 | ± 0.3 | 0.82 | ± 0.3 | 0.48 | 0.1 | 0.74 |
| 4 | 115.1 ± | $98.47 \pm$ | $90.9 \pm$ | 98.67 | $82.53 \pm$ | $72.8 \pm$ | 182 ± | 162.93 | $111.3 \pm$ |
| | 0.3 | 0.08 | 0.3 | ± 0.36 | 0.3 | 0.12 | 0.25 | ± 0.3 | 0.4 |
| 6 | 151.5 ± | $130.3 \pm$ | 157.87 | 128.4 | $105.6 \pm$ | 91.73 | 249 ± | 225.63 | $166 \pm$ |
| | 0.12 | 0.36 | ± 0.3 | ± 0.48 | 0.48 | ± 0.4 | 0.12 | ± 0.08 | 0.08 |
| 8 | 185 ± | 163.43 ± | 148.43 | 166.8 | 132.15 | 112.7 | $308.6 \pm$ | 290.21 | $222.6 \pm$ |
| | 0.74 | 1.32 | ± 1.42 | ± 2.23 | ± 0.1 | ± 1.66 | 0.74 | ± 1.36 | 1.986 |

Table 19: Results of cumulative drug release % in-vitro diffusion studies of hydrogel patch formulations

| Time | F1 | F2 | F3 | F4 | F5 | F6 | F7 | F8 | F9 |
|-------|---------|---------|---------|---------|---------|---------|---------|---------|---------|
| (h) | | | | | | | | | |
| 0.083 | 5.97142 | 3.88571 | 1.95142 | 6.83714 | 5.66571 | 3.45714 | 10.7914 | 8.28571 | 6.89714 |
| | 9 | 4 | 9 | 3 | 4 | 3 | 3 | 4 | 3 |
| 0.166 | 7.47 | 5.05142 | 2.38328 | 8.62757 | 6.85471 | 4.01 | 11.9681 | 8.98571 | 8.202 |
| | | 9 | 6 | 1 | 4 | | 4 | 4 | |
| 0.25 | 9.09428 | 9.98857 | 3.40328 | 10.3075 | 8.56328 | 5.10757 | 13.6738 | 10.3485 | 9.13771 |
| | 6 | 1 | 6 | 7 | 6 | 1 | 6 | 7 | 4 |
| 0.5 | 10.7932 | 11.6004 | 4.90571 | 12.2337 | 10.038 | 8.94471 | 18.5191 | 17.0385 | 10.6148 |
| | 9 | 3 | 4 | 1 | | 4 | 4 | 7 | 6 |
| 1 | 14.4875 | 14.2118 | 9.83528 | 15.3637 | 11.7265 | 11.1818 | 23.7495 | 20.0924 | 14.2391 |
| | 7 | 6 | 6 | 1 | 7 | 6 | 7 | 3 | 4 |

| 2 | 25.0965 | 22.1357 | 16.66 | 22.3684 | 19.0398 | 17.5757 | 31.4938 | 26.9828 | 21.2524 |
|---|---------|---------|---------|---------|---------|---------|---------|---------|---------|
| | 7 | 1 | | 3 | 6 | 1 | 6 | 6 | 3 |
| 4 | 36.2494 | 31.2238 | 27.8114 | 31.6494 | 26.4074 | 23.1295 | 57.0295 | 50.7614 | 35.0191 |
| | 3 | 6 | 3 | 3 | 3 | 7 | 7 | 3 | 4 |
| 6 | 48.2855 | 41.7248 | 48.2442 | 41.5532 | 34.1778 | 29.5781 | 78.7724 | 71.0032 | 52.2381 |
| | 7 | 6 | 9 | 9 | 6 | 4 | 3 | 9 | 4 |
| 8 | 60.0127 | 53.052 | 47.8024 | 54.359 | 43.2721 | 36.8771 | 99.3495 | 92.678 | 70.7757 |
| | 1 | | 3 | | 4 | 4 | 7 | | 1 |

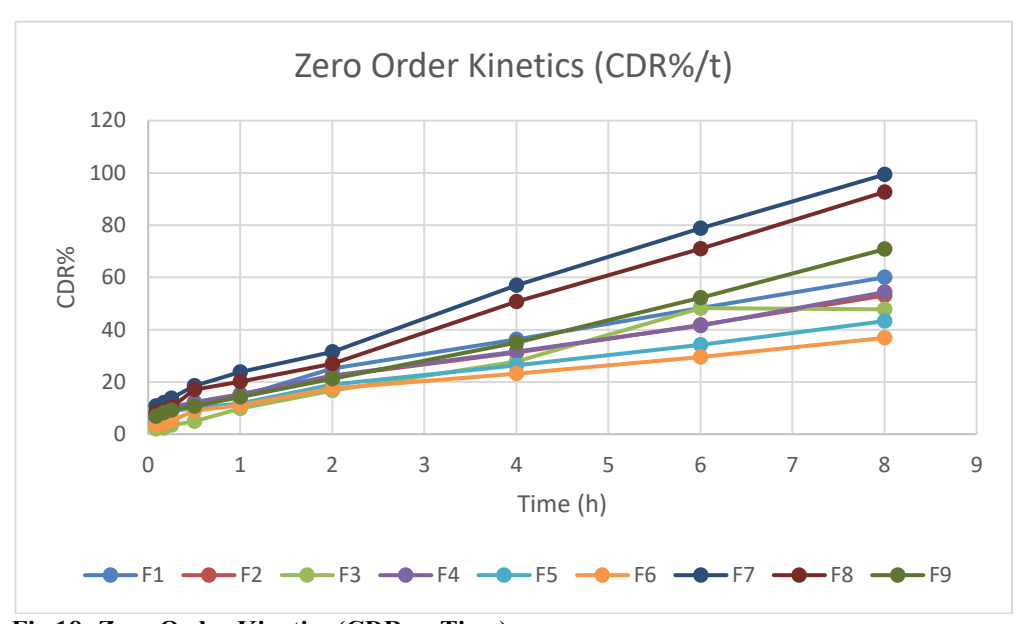


Fig 18: Zero Order Kinetics (CDR vs Time)

Table 20: Results of cumulative drug release % in-vitro diffusion studies of hydrogel patch formulation (F7)

| Parameter | In-vitro (F7) |
|-------------------------------|-------------------------------------|
| Initial Release (% at 5 min) | 10.79% |
| Cumulative Release (% at 8 h) | 99.35% |
| Best Kinetic Model | Zero Order (R ² =0.9982) |
| n value (Korsmeyer-Peppas) | 0.72 (Anomalous) |
| Release Rate Constant (k) | 0.237 |

Table 21: Results of drug release kinetics in-vitro diffusion studies of hydrogel patch formulations

| Model | In-vitro R ² (F7) |
|---------------------------------|------------------------------|
| Zero Order | 0.9982 |
| First Order | 0.7872 |
| Higuchi | 0.963 |
| Korsmeyer–Peppas R ² | 0.9575 |
| n (release exponent) | 0.72 |
| k (release rate) | 0.237 |

3.3.5 Ex-vivo Permeation Study

To simulate transungual delivery, ex-vivo studies were conducted using **freshly collected human volunteer nail clippings** (average thickness: 0.5-0.7 mm; surface area approx. 1.5 cm²), mounted on Franz diffusion cells. The hydrogel patch (F7) was applied on the dorsal surface of the nail, and receptor compartment contained phosphate buffer (pH 7.4) at 32 ± 0.5 °C.

Formulation F7 showed a cumulative drug permeation of 9.29% at 5 minutes, reaching 97.22% at 8 hours, indicating effective permeation through keratinized nail barrier.

• Kinetic Modeling (Ex-vivo Data):

The ex-vivo release profile for F7 showed highest R^2 value with **Zero Order kinetics** ($R^2 = 0.9978$). **Korsmeyer–Peppas model** indicated an **n-value of 0.524** and k = 0.267, again confirming **anomalous transport** and classifying it among the **fastest permeating formulations**.

Table 22: Results of cumulative drug release % ex-vivo permeation studies of hydrogel patch formulation (F7)

| Parameter | Ex-vivo (F7) |
|-------------------------------|-------------------------------------|
| Initial Release (% at 5 min) | 9.29% |
| Cumulative Release (% at 8 h) | 97.22% |
| Best Kinetic Model | Zero Order (R ² =0.9978) |
| n value (Korsmeyer-Peppas) | 0.524 (Anomalous) |
| Release Rate Constant (k) | 0.267 |

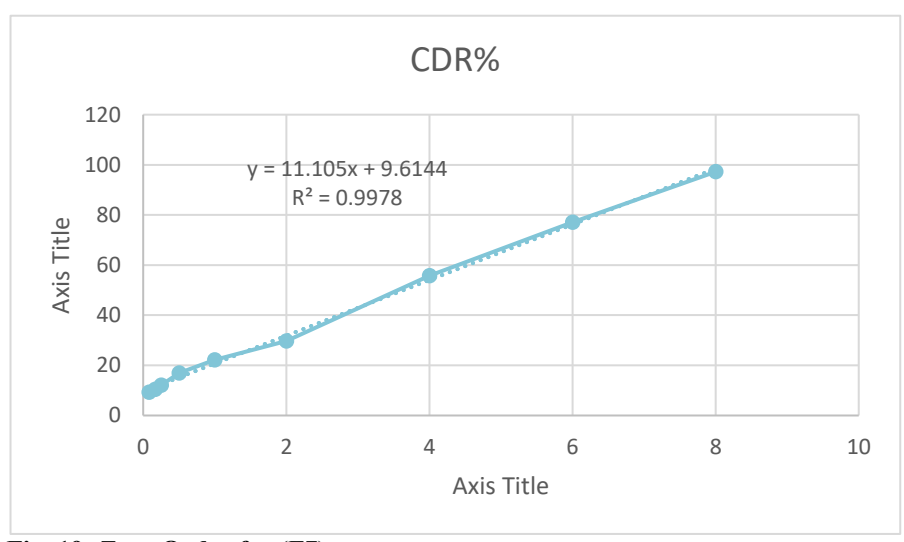


Fig 19: Zero Order for (F7)

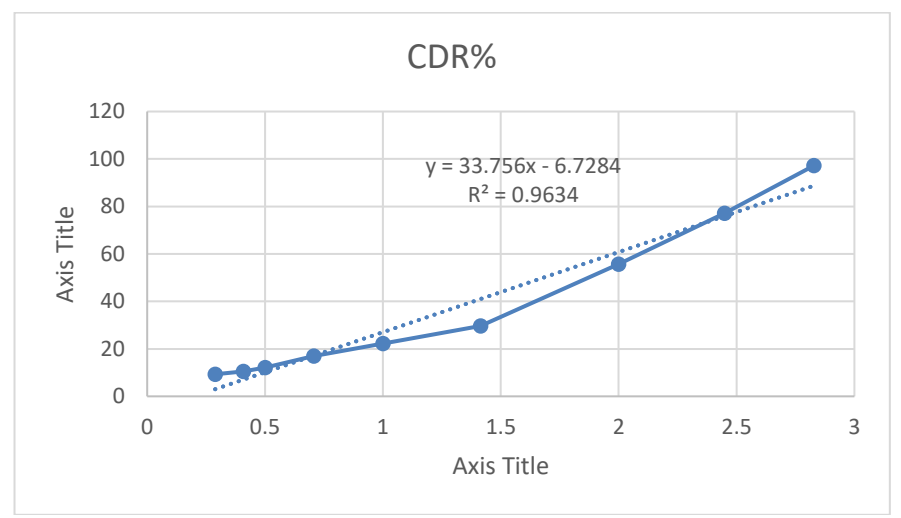


Fig 20: Higuchi Model (F7)

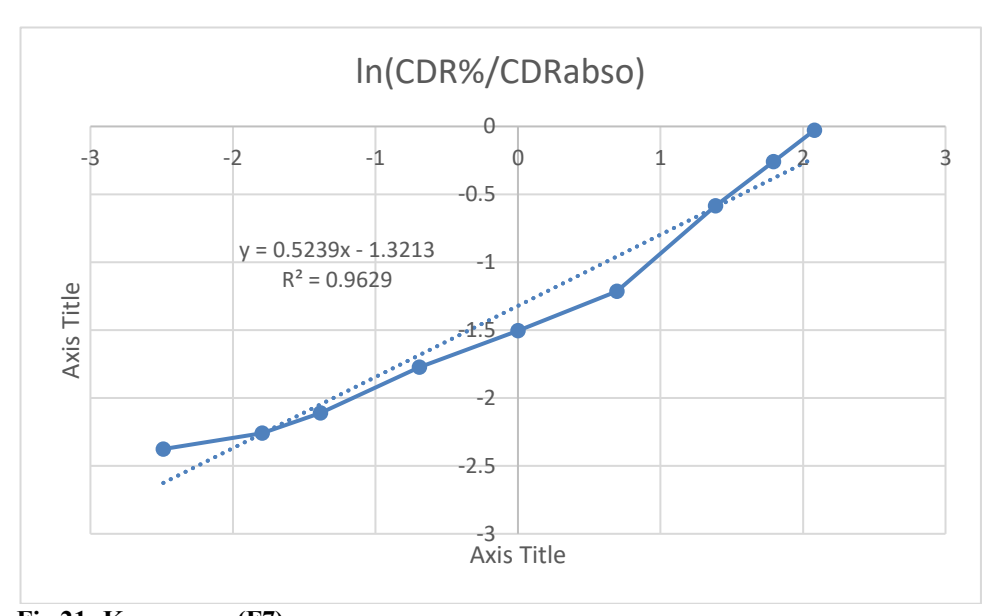


Fig 21: Korsmeyer (F7)

Table 23: Results of drug release kinetics ex-vivo permeation studies of hydrogel patch formulations

| Model | Ex-vivo R ² (F7) |
|---------------------------------|-----------------------------|
| Zero Order | 0.9978 |
| First Order | 0.8655 |
| Higuchi | 0.9634 |
| Korsmeyer–Peppas R ² | 0.9629 |
| n (release exponent) | 0.524 |
| k (release rate) | 0.267 |

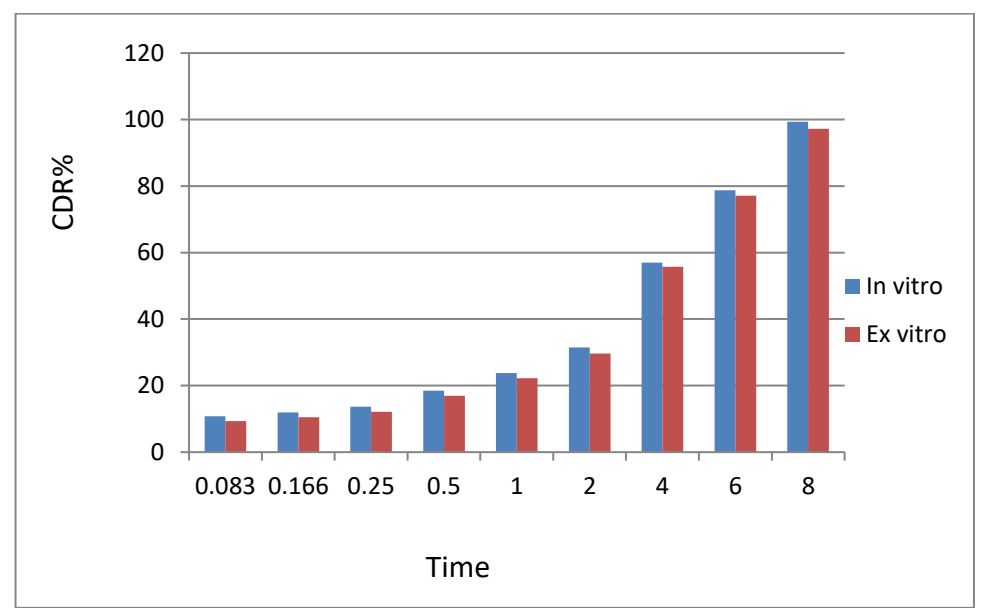


Fig 22: Comparison of In-vitro and Ex-vivo cumulative drug release (F7)

Fig 22 graph comparison of cumulative % drug release for Formulation F7 at key time intervals. It clearly shows how the in-vitro and ex-vivo profiles follow a similar sustained pattern, with slightly faster release in in-vitro conditions.

4. SUMMARY

This research addresses the persistent clinical challenge of onychomycosis—a fungal nail infection that affects millions globally—by innovating a transungual drug delivery system using nanosuspension-loaded hydrogel patches of terbinafine hydrochloride. Terbinafine, though a potent antifungal agent, is hindered by its poor water solubility and suboptimal topical bioavailability. By formulating the drug into nanosuspensions and embedding it within a bioadhesive hydrogel matrix, the study sought to enhance drug solubility, permeation, and therapeutic retention at the infection site.

High-pressure homogenization was employed to produce the nano suspension, which was then characterized for particle size, zeta potential, and solubility enhancement. Hydrogel patches were developed using Carbopol 934 and other pharmaceutical excipients to ensure mechanical strength, bioadhesion, and sustained release. Among the various batches tested, formulation F7 demonstrated optimal characteristics: uniform particle size (~372 nm), high drug content, excellent adhesiveness, and consistent drug distribution.

In-vitro and ex-vivo diffusion studies revealed that F7 followed zero-order kinetics, indicating a steady release rate, with over 99% drug release in 8 hours. Furthermore, the ex-vivo studies validated its effective penetration through the nail matrix, mimicking realistic application scenarios. Overall, this work provides a holistic framework for targeted, patient-compliant therapy against onychomycosis.

5. CONCLUSION

The study successfully demonstrates that a nano suspension-integrated hydrogel patch system can revolutionize transungual drug delivery by offering targeted, sustained, and non-invasive treatment of onychomycosis. The combination of particle size reduction and hydrogel encapsulation significantly enhances terbinafine's solubility and retention on the nail surface, overcoming major barriers posed by the dense keratinized structure of nails. Formulation F7 emerged as the most effective candidate,

displaying near-complete drug release and superior nail permeation within 8 hours—attributes essential for managing chronic fungal infections. The zero-order release pattern ensures predictable dosing and therapeutic consistency, while the anomalous diffusion mechanism highlights the interplay between drug diffusion and matrix swelling. Importantly, the pH compatibility and strong bioadhesion make the system suitable for long-term application without causing irritation or patient discomfort. This approach not only minimizes systemic side effects but also addresses the limitations of oral antifungals, especially for patients with hepatic concerns or polypharmacy. Furthermore, the research provides valuable insight into the application of nanotechnology and polymer science in transdermal systems, setting the groundwork for future innovations in localized drug delivery. In conclusion, the nano suspension-loaded hydrogel patch presents a promising, patient-friendly platform for effectively treating onychomycosis and possibly other nail disorders, redefining how antifungal therapies can be administered with enhanced precision, efficacy, and compliance.

6. REFERECES

- 1) Mirshekari, M., Bagheri Ghomi, A., & Mehravaran, A. (2021). Smart terbinafine recent nano-advances in delivery of terbinafine. Nanomedicine Journal, 8(4), 241–254.
- 2) Singh, A. (2022). The brief study on the human nail. International Journal of Innovative Research in Computer Science & Technology (IJIRCST), 10(2), 387–390.
- 3) Verma, S., Singh, R., & Ashima. (2016). Transungual drug delivery: A pivotal remedy in onychomycosis. Journal of Chemical and Pharmaceutical Research, 8(4), 370–381
- 4) Chiu, W. S. (2014). Visualization of the mechanism(s) of drug transport and delivery into and through the nail (Doctoral dissertation, University of Bath).
- 5) Gao, W., Vecchio, D., Li, J., Zhu, J., Zhang, Q., Fu, V., Li, J., Thamphiwatana, S., Lu, D., & Zhang, L. (2014). Hydrogel containing nanoparticle-stabilized liposomes for topical antimicrobial delivery. ACS Nano, 8(3), 2900–2907
- 6) Ghose, A., Nabi, B., Rehman, S., Md, S., Alhakamy, N. A., Ahmad, O. A. A., Baboota, S., & Ali, J. (2020). Development and evaluation of polymeric nanosponge hydrogel for terbinafine hydrochloride: Statistical optimization, in vitro and in vivo studies. Polymers, 12(12), 1–19
- Rajendra, V. B., Baro, A., Kumari, A., Dhamecha, D. L., Lahoti, S. R., & Shelke, S. D. (2012). Transungual drug delivery: An overview. Journal of Applied Pharmaceutical Science, 2(1), 203–209.
- 8) DrugBank Online. (n.d.). Terbinafine DrugBank ID: DB00857.
- 9) Darkes MJ, Scott LJ, Goa KL: Terbinafine: a review of its use in onychomycosis in adults. Am J Clin Dermatol. 2003;4(1):39-65.
- 10) Phaechamud, T., & Tuntarawongsa, S. (2016). Transformation of eutectic emulsion to nanosuspension fabricating with solvent evaporation and ultrasonication technique. Asian Journal of Pharmaceutical Sciences, 11(2), 2855–2865.
- 11) Jassim, Z. E., & Rajab, N. A. (2018). Review on preparation, characterization, and pharmaceutical application of nanosuspension as an approach of solubility and dissolution enhancement. Journal of Pharmacy Research, 12(5), 771–774.
- 12) Gao, W., Vecchio, D., Li, J., Zhu, J., Zhang, Q., Fu, V., Li, J., Thamphiwatana, S., Lu, D., & Zhang, L. (2014). Hydrogel containing nanoparticle-stabilized liposomes for topical antimicrobial delivery. ACS Nano, 8(3), 2900–2907.
- 13) Kaur, M., Choudhary, A., Upadhyay, P., Khujar, S., Gupta, N. B., & Sharma, P. (2020). Formulation and evaluation of Imiquimod loaded nanosuspension gel for transdermal delivery. International Journal of Pharmacy & Pharmaceutical Research, 17(4), 1–15.
- 14) Afzal, S., Barkat, K., Ashraf, M. U., Khalid, I., Mehmood, Y., Shah, N. H., Badshah, S. F., Naeem, S., Khan, S. A., & Kazi, M. (2023). Formulation and characterization of polymeric cross-linked hydrogel patches for topical delivery of antibiotic for healing wound infections. Polymers (Basel), 15(7), 1652.

- 15) Franklin, L. (2013, January 1). Commentary on nails. Brill's Annual of Papyrology, 28(1), 102–109.
- 16) Cooper, A. (1827, April). Observations on the anatomy and diseases of the nails. London Medical and Physical Journal, 2(10), 289–291.
- 17) Tucker, J. R. J. (2015, December). Nail deformities and injuries. Primary Care, 42(4), 677–691.
- 18) Dhingra, G., Ahmad, N., Tanwar, S., Goyal, S., & Chaturvedi, V. (2022, August 15). Nail disorders: An updated review. International Journal of Pharmaceutical Sciences Review and Research, 135–144.
- 19) ResearchGate. (2025). Nail disorders: An update review. ResearchGate Publication.
- 20) Bernier, V., Labrèze, C., Bury, F., & Taïeb, A. (2001, November). Nail matrix arrest in the course of hand, foot and mouth disease. European Journal of Pediatrics, 160(11), 649–651.
- 21) Haneke, E. (2015, June). Anatomy of the nail unit and the nail biopsy. Seminars in Cutaneous Medicine and Surgery, 34(2), 95–100.
- 22) Hirata, S. H., Yamada, S., Almeida, F. A., Enokihara, M. Y., Rosa, I. P., Enokihara, M. M. S., et al. (2006, January). Dermoscopic examination of the nail bed and matrix. International Journal of Dermatology, 45(1), 28–30.
- 23) Iorizzo, M., Starace, M., Di Altobrando, A., Alessandrini, A., Veneziano, L., & Piraccini, B. M. (2021, December). The value of dermoscopy of the nail plate free edge and hyponychium. Journal of the European Academy of Dermatology and Venereology, 35(12), 2361–2366.
- 24) Daughters, D. B., & Maibach, H. (1976, January 1). Exaggerated onychodermal band associated with unilateral racket thumb nail. Acta Dermato-Venereologica, 56(1), 73–75.
- 25) Scheinfeld, N., Dahdah, M. J., & Scher, R. (2007, August). Vitamins and minerals: Their role in nail health and disease. Journal of Drugs in Dermatology, 6(8), 782–787.
- 26) Chauhan, S., D'Cruz, S., Singh, R., & Sachdev, A. (2008, October 18). Mees' lines. The Lancet, 372(9647), 1410.
- 27) Palmou, N., Marzo-Ortega, H., Ash, Z., Goodfield, M., Coates, L. C., Helliwell, P. S., et al. (2011). Linear pitting and splinter haemorrhages are more commonly seen in the nails of patients with established psoriasis in comparison to psoriatic arthritis. Dermatology, 223(4), 370–373.
- 28) Zaias, N., Escovar, S. X., & Zaiac, M. N. (2015, May). Finger and toenail onycholysis. Journal of the European Academy of Dermatology and Venereology, 29(5), 848–853.
- 29) Albright, S. D., III, & Wheeler, C. E., Jr. (1964, October 1). Leukonychia: Total and partial leukonychia in a single family with a review of the literature. Archives of Dermatology, 90(4), 392–399.
- 30) Braswell, M. A., Daniel, C. R., & Brodell, R. T. (2015, November). Beau lines, onychomadesis, and retronychia: A unifying hypothesis. Journal of the American Academy of Dermatology, 73(5), 849–855.
- 31) Walker, J., Baran, R., Vélez, N., & Jellinek, N. (2016, November). Koilonychia: An update on pathophysiology, differential diagnosis and clinical relevance. Journal of the European Academy of Dermatology and Venereology, 30(11), 1985–1991.
- 32) Kawabata, Y., Kwada, K., Nakatani, M., Yamada, S., & Onoue, S. (2011). Formulation design for poorly water-soluble drugs based on biopharmaceutics classification system: Basic approaches and practical applications. International Journal of Pharmaceutics, 420(1), 1–10.
- 33) Kumar, S., & Singh, P. (2016). Various techniques for solubility enhancement: An overview. Pharma Innovation Journal, 5(1), 23–28.
- 34) Wang, Y., Zheng, Y., Zhang, L., Wang, Q., & Zhang, D. (2013). Stability of nanosuspensions in drug delivery. Journal of Controlled Release, 172(3), 1126–1141.
- 35) Shen, C., Shen, B., Liu, X., & Yuan, H. (2018). Nanosuspensions based gel as delivery system of nitrofurazone for enhanced dermal bioavailability. Journal of Drug Delivery Science and Technology, 43, 1–11.

- 36) Jane, M., Agrawal, S., & Khan, A. (2018). Formulation and evaluation of nanosuspension of valsartan. International Journal of Current Pharmaceutical Research, 10(2), 68–74.
- 37) Bhalekar, R. M., Madgulkar, R. A., & Shaikh, G. S. (2018). Formulation and evaluation of chitosan-based mucoadhesive buccal patch of prochlorperazine maleate. International Journal of Pharmacy and Pharmaceutical Research, 12(4), 61–73.
- 38) Vinod, K. R., Santhosha, D., & Anbazhagan, S. (2011). Formulation and evaluation of piperine cream: A new herbal dimensional approach for vitiligo patients. International Journal of Pharmacy and Pharmaceutical Sciences, 3(2), 29–33.
- 39) Pandey, N., Sah, A. N., & Mahara, K. (2016). Formulation and evaluation of floating microspheres of nateglinide. International Journal of Pharmaceutical Sciences and Research, 7, 453–464.
- 40) Jassem, N. A., & Rajab, N. A. (2017). Formulation and in vitro evaluation of azilsartan medoxomil nanosuspension. International Journal of Pharmacy and Pharmaceutical Sciences, 9(7), 110–119.